Received: 27 September 2018 | Revised: 24 February 2019 | Accepted: 25 February 2019

DOI: 10.1002/aoc.4913

FULL PAPER

WILEY Applied Organometallic Chemistry

Novel 3-Hydroxy-2-naphthoic hydrazone and Ni(II), Co(II) and Cu(II) Complexes: Synthesis, Spectroscopic Characterization, Antimicrobial, DNA Cleavage and Computational Studies

Anthony C. Ekennia[1] | Elochukwu C. Ibezim[2] | Obinna C. Okpareke[2,3] | Collins U. Ibeji[2,4] | Chigozie J.O. Anarado[5] | Ilknur Babahan[6] | Burak Coban[7] | Bahruz Abulhasanov[7] | Füsun Cömert[8] | Oguejiofo T. Ujam[2]

[1]Department of Chemistry, Alex Ekwueme Federal University Ndufu-Alike (AE-FUNAI), Ikwo, P.M.B 1010, Abakaliki, Ebonyi State, Nigeria

[2]Department of Pure and Industrial Chemistry, Faculty of Physical Sciences, University of Nigeria, Nsukka 410001Enugu State, Nigeria

[3]Department of Chemistry, University of Waikato, Private Bag 3105, Hamilton, New Zealand

[4]Catalysis and Peptide Research Unit, School of Health Sciences, University of KwaZulu-Natal, Durban 4041, South Africa

[5]Department of Pure and Industrial Chemistry, Nnamdi Azikwe University, Awka, Anambra State, Nigeria

[6]Department of Chemistry, Adnan Menderes University, Aydin 09010, Turkey

[7]Department of Chemistry, Faculty of Arts and Sciences, Zonguldak Bulent Ecevit University, Zonguldak 67100, Turkey

[8]Department of Microbiology, Faculty of Medicine, Zonguldak Bulent Ecevit University, Zonguldak 67100, Turkey

Correspondence
Oguejiofo T. Ujam, Department of Pure and Industrial Chemistry, Faculty of Physical Sciences, University of Nigeria, Nsukka 410001, Enugu State, Nigeria.
Email: oguejiofo.ujam@unn.edu.ng

A novel hydrazone ligand derived from condensation reaction of 3-hydroxy-2-naphthoic hydrazide with dehydroacetic acid, and its Ni(II), Cu(II) and Co(II) complexes were synthesized, characterized by spectroscopic, elemental analyses, magnetic susceptibility and conductivity methods, and screened for antimicrobial, DNA binding and cleavage properties. Spectroscopic analysis and elemental analyses indicated the formula, $[MLCl_2]$, for the complexes; square planar geometry for the nickel, and tetrahedral geometry for copper and cobalt complexes. The non-electrolytic natures of the complexes in Dimethyl Sulphoxide (DMSO) were confirmed by their molar conductance values in the range of 6.11–14.01 $\Omega^{-1}cm^2mol^{-1}$. The copper complex had the best antibacterial activity against *Staphylococcus aureus* (ATCC 29213). DNA cleavage activities of the compounds, evaluated on pBR322 DNA, by agarose gel electrophoresis, in the presence and absence of oxidant (H_2O_2) and free radical scavenger (DMSO), indicated no activity for the ligand, and moderate activity for the complexes, with the copper complex cleaving pBR322 DNA more efficiently in the presence of H_2O_2. When the complexes were evaluated for antibacterial and A-DNA activity using Molecular docking technique, the copper complex was found to be most effective against Gram-positive (*S. aureus*) bacteria. $[CuLCl_2]$ showed good hydrogen bonding interaction with the major-groove (C_2·G_{13} base pair) of A-DNA. Density functional theory (DFT) calculations of the structural and electronic properties of the complexes revealed that $[CuLCl_2]$ had a smaller HOMO-LUMO gap, suggesting a higher tendency to donate electrons to electron-accepting species of biological targets.

KEYWORDS
antimicrobial and DNA binding, complexes, Dehydroacetic acid, Naphthoic hydrazone

1 | INTRODUCTION

Hydrazones derived from naphthoic hydrazide moiety are extensively investigated due to the rich chemistry they exhibit.[1–3] They find applications as synthetic precursors to many bioactive compounds[2,4–6] that exhibit antimicrobial activity[5,7–9] and significant antiproliferative activity against human cancer cell lines.[2,4] Due to their good ligating abilities towards metal ions, they are also used in the preparation of structurally interesting coordination compounds,[1,3,10] and therefore, can potentially be employed in metal chelation therapy. In general, hydrazones are mainly synthetically accessible by facile condensation reaction between hydrazides and appropriate carbonyls. This reaction has been employed in biochemical analysis. For instance, 3-hydroxy-2-naphthoic acid hydrazide is reportedly used in quantification of histochemical stains in carbonyls, through its facile reaction with acyl groups in DNA, to form reactive hydrazones, which couple with Fast Blue B.[11] Within this reactivity framework lies a large unutilized landscape for generating novel, uninvestigated, potential bio-friendly drug-target molecules, with moderate side effects.

Molecules with pyran-2-one core/nucleus constitute large family of biologically active compounds.[12–14] Small changes, by substitution pattern, on the 2-pyrone ring often lead to diverse biological properties.[13,15] For instance, 4-hydroxy-2-pyrones are considered as one important class of anti-HIV agents. Among the derivatives of pyran-2-one, dehydroacetic acid has been used as reactant in the synthesis of heterocyclic compounds,[16–20] and many of its derivatives form uniquely important class of bioactive compounds.[21–23] They exhibit wide range of antifungal, phytotoxic, antibacterial, cytotoxic and neurotoxic activities.[24–28] Their metal complexes have also been investigated for applications as therapeutic agents against bacteria, based on selective DNA cleavage ability.[14,29]

It may ordinarily be expected that hydrazone derived from the condensation or combination of a naphthoic hydrazide and dehydroacetic acid would exhibit reasonable biological activity, but to the best of our knowledge, there is no such report in literature. In addition, the bioactivity of drug molecules can be altered when coordinated to metal ions. Preliminary step in the design of new DNA-targeted drugs and their *in-vitro* screening via pre-investigation of the interaction between DNA and potential drug molecules, is a very important subject of interest.[30–32] In this contribution, we report the synthesis and characterization of a novel hydrazone ligand, 3-hydroxy-*N*′-[(1*Z*)-1-(4-hydroxy-6-methyl-2-oxo-2*H*-pyran-3-yl)ethylidene]naphthalene-2-carbohydrazide, the Ni(II), Cu(II), Co(II), complexes, by conventional spectroscopic techniques, anti-microbial and DNA binding activities tests. Molecular docking was used to establish the interaction of the molecules with different drug targets, and DNA binding activities. It was also used to determine possible binding interaction of the complexes with gram-negative and gram-positive bacteria, and DNA binding activities. Furthermore, to complement the experimental results, the structural geometries of the complexes were confirmed by Density Functional Theory (DFT) calculations, and as such, their electronic and thermodynamic properties were explored via reported protocol.[33,34]

2 | EXPERIMENTAL

2.1 | Materials

Analar grade 3-hydroxy-2-naphthoichydrazide, 3-acetyl-2-hydroxy-6-methyl-4H-pyran-4-one (dehydroacetic acid), glacial acetic acid, triethylamine, cobalt(II) chloride hexahydrate, anhydrous copper(II) chloride and nickel(II) chloride were bought from Sigma–Aldrich, and were used as received. Ethanol, methanol and DMSO were obtained from local suppliers, and redistilled before use. Solutions of calf thymus DNA (CT-DNA, purchased from Sigma) in 50 mM ammonium acetate (pH 7.5) had a UV–Vis absorbance ratio of 1.8–1.9: 1 at 260 and 280 nm (A_{260}/A_{280} = 1.9), indicating that the DNA was sufficiently free of protein. The concentration of the DNA was determined spectrophotometrically, using a molar absorptivity of 6600 M^{-1} cm^{-1} (260 nm).[35] Double-distilled water was used to prepare buffers. Stock solution of the CT-DNA was stored at 4 °C, and was used within 4 days.

2.2 | Physical methods

The infrared spectra of the compounds were obtained with KBr disc on a Bruker alpha-P FTIR spectrophotometer. The Nuclear Magnetic Resonance (NMR) analyses were carried out using a 400 MHz-Bruker Avance III NMR spectrophotometer. Micro elemental analyses for C, H, N of the compounds were obtained with Elementar, Vario EL Cube set-up for CHN analysis. The electronic spectra were recorded on a Perkin-Elmer K20-UV–Vis spectrophotometer. The magnetic susceptibility measurements were made using Sherwood Susceptibility balance, MSB Mark 1. Molar conductance measurements were done with Hanna, H19991300 conductivity meter. Electrospray ionization-mass spectrometry (ESI-MS) studies of the solid products were done by dissolving small quantity of the material in 1–2 ml of 1:1 solution

of DMSO/DMF, followed by dilution to ca. 2 mL using methanol. The mass spectra were recorded on a Waters Micromass Q-TOF II Mass Spectrometer, in positive ion mode, using pneumatically assisted electrospray ionization: capillary of voltage, 2900 V; sample cone voltage, 15 V; extraction voltage, 1 V; source temperature, 80 °C; desolvation temperature, 160 °C; cone gas flow, 100Lh $^{-1}$; desolvation gas flow, 100Lh^{-1}; collision voltage, 2 V; MCP voltage, 2400 V. No smoothening of the data was performed, and comparison of observed and calculated isotope patterns[36,37] was used in the ion assignment.

2.3 | UV titrations

The absorption titrations was done according to literature procedure.[35,38] The ligand and complexes (about 1 mmol) were dissolved in a minimum amount of DMSO (0.5 ml), and were then diluted in buffer (5 mM ammonium acetate, pH 7.5), to a final concentration of 20 μM. Titrations were performed in a 10 mm-stoppered quartz cell, by using a mixed concentration of the complex (20 μM), to which the CT-DNA stock solution was added, in increments of 2 μL, till no change in absorption spectrum. The analysis was performed by means of a UV–Vis spectrophotometer, by recording the spectrum after each addition of DNA. The ligand or complex–DNA solutions were mixed by using a Pasteur pipette, and were incubated for 10 minutes, each time, before the spectra were recorded. The cell compartments were thermostated at 25 ± 0.1 °C. The stabilities of the ligand and complex solutions were tested by measuring the change in absorption for 1 hr, with 15 min intervals.

2.4 | Gel electrophoresis

Gel electrophoresis experiments were performed according to reported procedure,[35,39] using pBR322 negatively supercoiled plasmid DNA on 1% agarose gels, by using a tris–borate–EDTA-running buffer solution. Reaction mixtures (10 μL) containing 0.1 μg of pBR322, together with different amounts of the complexes (1, 10, 100 μM) were prepared in 50-mM ammonium acetate buffer, pH 7.5 at 0 °C, and then allowed to incubate at 36 °C for 1 hr, in the dark, then in the presence of peroxide solution. Prior to loading samples onto the gel, 2.5 ml of 0.25% bromophenol blue, loading buffer, and sucrose-in-water (40% *w*/*v*) were added to the reaction mixtures. Gels were obtained at room temperature, by using a Thermo midi horizontal agarose gel electrophoresis system, and applying a potential of 35 V for 4 h. The resulting gels were stained in EB solution (0.5 mg ml^{-1}) for 45 min, after which they were soaked in water for a further 20 min. Gels were visualized under UV light and photographed.

2.5 | Antimicrobial susceptibility

Antimicrobial susceptibility to the ligand and complexes was determined by Micro-broth dilution method,[40] as recommended by the European Committee on Antimicrobial Susceptibility Testing (EUCAST). The stock solutions were prepared in DMSO, at 500 mg μL^{-1}, and serial two-fold dilution of each chemical complex (totaling 10 dilutions between 250–0.48 mg μL^{-1}), were prepared with the cation-adjusted Mueller-Hinton broth (CAMHB) in sterile 96-well polystyrene U-bottom broth micro-dilution trays. *Staphylococcus aureus* ATCC 29213, *Enterococcus faecalis* (ATCC 29212), *Escherichia coli* (ATCC 25922) and *Pseudomonas aeruginosa* (ATCC 27853) were used (10^4 CFU/well) as test microorganisms. Cefotaxime was used as the control antimicrobial agent. The lowest concentration of the chemical complexes and antimicrobial agent demonstrating complete inhibition of growth was determined as minimal inhibitor concentration (MIC). The tests were repeated.

3 | COMPUTATIONAL DETAILS

3.1 | Molecular docking

Molecular docking was carried out, to determine the binding affinities of the complexes using AutoDock Vina software.[41] The crystal structure of the DNA was retrieved from protein data bank (PDB), with access code: 3V9D,[42] (resolution, 2.5 Å), The right-hand double-helix A-DNA with more compact conformation was used for the docking. The crystal structures of *Staphylococcus aureus* (PDB: 2DHN, with 2.2 Å resolution),[43] *Enterococcus faecalis* (PDB: 5y63, with 2.8 Å resolution),[44] *Escherichia coli* (PDB: 1wxh, with 1.97 Å resolution)[45] and *Pseudomonas aeruginosa* (PDB: 2w7q, with 1.88 Å resolution)[46] were retrieved from PDB database. These proteins were selected based on the reported interactions with their respective native ligands, the well defined crystal structures and the resolutions.

The structural preparation of the DNA, gram-positive and -negative bacteria was done with Discovery studio visualize, V16.[47] (Note: Please renumber accordingly)[45] AutoDock Tools[48] 1.5.4. was used to define the active site, with appropriate grid box size of X = 20, Y = 20, Z = 20, and 1.00 Å as the grid spacing for A-DNA, and 40x40x40 for bacteria. Gasteiger charges were added using the AutoDock Tools graphical user-interface, supplied by MGL Tools.[49] The metal complexes were

optimized, using Gaussian 09,[50] prior to docking, to obtain the global minimal structures.[51,52]

3.2 | DFT calculations

Geometry optimization was performed for L, [$CuLCl_2$], [$CoLCl_2$] and [$NiLCl_2$], using density functional theory (DFT) Becke 3 Lee Yang par[53] (B3LYP), in conjunction with 6–31 + G(d,p) basis-set for all atoms, except for metal ions. LANL2DZ basis-set was used for metal ions (Cu, Co and Ni). The combination of B3LYP/6–31 + G(d,p)/LANL2DZ[54] has been reported to be effective and suitable for calculations involving metal complexes.[55–57] Frontier molecular orbital (FMO), referred to as the highest occupied molecular orbital (HOMO), and the lowest unoccupied molecular orbital (LUMO), were determined (reactivity index).[58,59] To obtain the fundamental thermodynamic properties, frequency calculation was performed.

^{1}H magnetic shielding constants, obtained on a δ-scale, comparative to the TMS(reference), were determined using the Gauge-Independent Atomic Orbital (GIAO) method, developed by Wolinski et al.[60] Polarizable Continuum Model (PCM),[61] through a single-point (B3LYP/6–311 + G(2d,p)) calculation,[62] was applied to calculate the ^{1}H NMR chemical shift (DMSO-d_6), solvent: dielectric constant, ε = 46.826). All calculations were carried out using Gaussian 09.[50]

The enthalpy (ΔH), Gibb's free energy (ΔG) and entropy (ΔS) were calculated, according to following expression[54,63]:

$$M(II) + mL_i + nL_j + + + \quad \leftrightarrow \quad M - L_{complex} \qquad (1)$$

M(II) represents the Cu(II), Co(II) and Ni(II) ; L_i, L_j are the coordinated ligands; *m and n* are the numbers of moles of the ligands.

3.3 | Synthesis

Synthesis of (*E*)-3-Hydroxy-*N*′-(1-(6-methyl-2,4-dioxo-3,4-dihydro-2*H*-pyran-3-yl)ethyli dene)-2-naphthohydrazide (L).

A 30 mL-methanol solution of 3-acetyl-2-hydroxy-6-methyl-4H-pyran-4-one (1000 mg, 5 .9 mmol) was added to an equimolar solution of 3-hydroxy-2-naphthoic hydrazide (1201 mg, 5.9 mmol), drop-wise, and stirred. Three drops of glacial acid were added after five minutes, and the solution refluxed for 4 hr. The resulting cream-colored precipitates were filtered, re-crystallized in hot methanol, and stored over silica gel, under vacuum.

Yield: 75%; m.p: 259-261 °C; Selected IR data (KBr, ν/cm^{-1}): 3472b ν(O-H str), 3325 s, 3416 s, ν(N-H str), 3058 s ν (aromatic C-H str), 2852 m, 2922 m ν (aliphatic C-H str), 1713s, 1672, ν(C=O str), 1649s ν (bending N-H), 1628s ν(C=N), 1603s, 1554s ν(C=C str), 1318s, 1262s ν(C-N str), 1220s, 1236s ν(C-O str). ^{1}H NMR (400 MHz, DMSO-d_6): 2.15 (s, H_{15}), 2.66 (s, H_{14}), 3.37 (2OH), 5.94 (s, H_5), 8.49–7.34 (m, Ar-CH naphthene, $H_{16–25}$), 11.10 (s, H_{26}) ppm. ^{13}C{H} NMR (100 MHz, DMSO-d_6): 181.51 (C_4), 168.53 (C_8), 163.74 (C_2), 162.84 (C_{11}), 153.50 (C_6), 136.41 (C_5), 132.00 (C_{17}), 105.98–129.29 ($C_{16–25}$), 95.31(C_3), 17.16 (C_{15}), 19.77 (C_{14}). ESI-MS (*m*/*z*): 353 ([M + H]$^+$, 100%, 375 [M + Na]$^+$, 70%), 391 [M + K]$^+$ 39%), Cal. = 352.338. Anal. Calc. for $C_{19}H_{16}O_5N_2$ (352.338): C, 64.77; H, 4.58; N, 7.95. Found: C, 64.78; H, 4.58; N, 7.95%; UV–visible (λ_{max}, DMSO, nm): 229, 247 (π → π*), 344 (n → π*).

3.4 | Synthesis of Metal(II) Complexes of 3-Hydroxy-*N*′-[(1*Z*)-1-(4-hydroxy-6-methyl-2-oxo-2*H*-pyran-3-yl)ethylidene] naphthalene-2-carbohydrazide.

The metal complexes were prepared by reacting 1:1 stoichiometric ratio of the ligand and metal salts. A methanol-solution of the respective metal salts ($NiCl_2$, $CuCl_2$ and $CoCl_2.6H_2O$) was added to 15 mL-solution of the hydrazone (40 mg, 1.14 mmol), while stirring. The reaction was buffered with triethylamine, and refluxed for 4 hr. The resulting precipitates were filtered off, washed with cold methanol, recrystallized in hot methanol and dried in vacuum.

3.5 | [$CuLCl_2$]

Yield: 83%; m.p: 346-348 °C; Selected IR data (KBr, ν/cm^{-1}): 3411 s ν(O-H str), 3051 s ν (aromatic C-H str), 2798 m, 2850 m, 2924 m ν (aliphatic C-H str), 1679, ν(C=O str), 1635s ν(C=N), 1589s, 1574s, 1543s ν(C=C str), 1311s, 1354s ν(C-N str), 1223s, 1237s ν(C-O str), 477 s, ν(M-O str), 502 s, 542 s ν(M-N str). ESI-MS (*m*/*z*): ([M]$^+$, 100%) = 487.0355 (Cal. = 486.887). Anal. Calc. for $CuC_{19}H_{16}O_5N_2Cl_2$ (486.848): C, 46.87; H, 3.31; N, 5.76. Found: C, 46.88; H, 3.33; N, 5.77%. UV–visible (λ_{max}, DMSO, nm): 243 (π → π*), 302 (n → π*), 404 (d-d). μeff (BM): 1.98. Molar conductance ($\Omega^{-1}cm^2mol^{-1}$): 6.11.

3.6 | [$CoLCl_2$]

Yield: 80%; m.p: 354–356 °C; Selected IR data (KBr, ν/cm^{-1}): 3414 s ν(O-H str), 3232 s, ν(N-H str), 3057 s ν

(aromatic C-H str), 2714 m, 2854 m, 2922 *ν* (aliphatic C-H str), 1711s, 1673, *ν*(C=O str), 1630s *ν*(C=N), 1605s, 1547s *ν*(C=C str), 1364s, 1393s *ν*(C-N str), 1220s, 1234 *ν*(C-O str), 482, *ν*(M-O str), 508 s, 574 s, *ν*(M-N str). ESI MS (m/z): ($[M]^+$, 100%) = 483 (Cal. = 482.181). Anal. Calc. for $CoC_{19}H_{16}O_5N_2Cl_2$ (482.268): C, 47.32; H, 3.34; N, 5.81. Found: C, 47.36; H, 3.36; N, 5.83%. UV–visible (λ_{max}, DMSO, nm): 229 ($\pi \rightarrow \pi^*$), 361, 378 ($n \rightarrow \pi^*$), 405 ($^4A_2 \rightarrow {}^4T_1(F)$ transition). μeff (BM): 4.35. Molar conductance ($\Omega^{-1}cm^2mol^{-1}$): 11.56.

3.7 | [$NiLCl_2$]

Yield: 60%; m.p: 202–204 °C; Selected IR data (KBr, v/cm^{-1}): 3413 s *ν*(O-H str), 3270 s *ν*(N-H str), 3056 s *ν* (aromatic C-H str), 2856 m, 2922 m, 2960 *ν* (aliphatic C-H str), 1678, *ν*(C=O str), 1636s *ν*(C=N), 1609s, 1543s *ν*(C=C str), 1358s *ν*(C-N str), 1226s *ν*(C-O str), 481 s, *ν*(M-O str), 527 s, 575 s, *ν*(M-N str). ^{1}H NMR (400 MHz, DMSO-d_6): 2.12 (s, H_{15}), 2.68 (d H_{14}), 3.06 (OH), 5.85 (H_{10}), 8.48–7.04 (m, Ar-CH naphthene, $H_{16–25}$), 11.08 (NH) ppm. ESI-MS (*m/z*): ($[M]^+$, 100%) = 482.048 (Cal. = 482.034). Anal. Calc. for $NiC_{19}H_{16}O_5N_2Cl_2$ (481.848): C, 47.36; H, 3.35; N, 5.76. Found: C, 47.40; H, 3.36; N, 5.78%. UV–visible (λ_{max}, DMSO, nm): 245 ($\pi \rightarrow \pi^*$), 391 ($n \rightarrow \pi^*$), 414 ($^1Ag \rightarrow {}^1Eg$ transition). μeff (BM): 0.14. Molar conductance ($\Omega^{-1}cm^2mol^{-1}$): 14.01.

4 | RESULTS AND DISCUSSION

4.1 | General synthesis

The ligand formation, according to reported procedures, involved the nucleophilic attack of the primary amine (3-hydroxy-2-naphthoic hydrazide) on one of the carbonyl carbon atoms (C_8) of 3-acetyl-2-hydroxy-6-methyl-4H-pyran-4-one, in an alcohol medium, to give the ligand (Scheme 1).[1] The reaction of the ligand with Co(II), Ni(II) and Cu(II) chlorides afforded the three metal complexes (Scheme 2). The compounds were characterized by

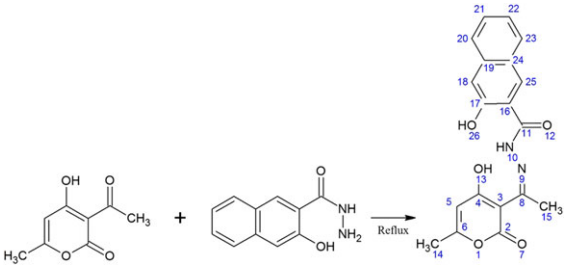

SCHEME 1 Synthesis of 3-hydroxy-*N*′-[(1*Z*)-1-(4-hydroxy-6-methyl-2-oxo-2*H*-pyran-3-yl)ethylidene]naphthalene-2-carbohydrazide (**L**)

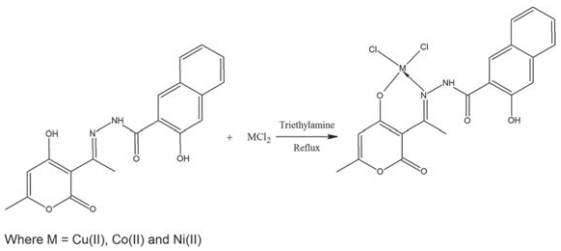

SCHEME 2 Synthesis of Metal(II) Complexes of 3-Hydroxy-*N*′-[(1*Z*)-1-(4-hydroxy-6-methyl-2-oxo-2*H*-pyran-3-yl)ethylidene] naphthalene-2-carbohydrazide

NMR, mass spectrometry, IR and UV–Vis spectroscopies, elemental analysis, magnetic susceptibility and molar conductance measurements.

4.2 | ^{1}H and ^{13}C-NMR spectra of the ligand (L) and [$NiLCl_2$]

The ^{1}H and ^{13}C-NMR spectra of the ligands are presented as supplementary materials (S1–**2)**. The ^{1}H-NMR spectrum of the ligand showed a singlet peak at 11.10 ppm, due to proton of the hydroxyl group. The appearance of this peak in the spectrum of the nickel complex indicates the non-deprotonation and non-involvement of the hydroxyl group in the coordination. The singlet peak at 5.94 ppm was ascribed to proton of the secondary amine group in the ligand, and was observed in the spectrum of [$NiLCl_2$]. This is due to the non-deprotonation and non-participation of the amine group in chelation. The protons of the methyl groups were seen as singlets at 2.66 and 2.16 ppm in the spectrum of the compounds. Aromatic C-H of the naphthene ring gave peaks within the range of 8.49–7.34 ppm in the spectrum of the ligand. The ^{13}C-NMR spectrum of the ligand was used to corroborate the inferences drawn from the proton-NMR spectrum. The carbon atoms of the carbonyl groups were seen at 181.51 and 168.53, 162.68 ppm. The carbon atom of the azomethine group presented a peak at 162.84 ppm, which is indicative of the formation of the hydrazone ligand.[64] The carbon atoms of the naphthene ring were observed at 105.98–129.29 ppm. Carbon atoms of the methyl groups were assigned to the peaks at 17.16 and 19.77 ppm.

4.3 | Mass spectra and elemental analysis

The mass spectra of the ligand and its metal complexes are presented as supplementary materials (**S3–S6**). The molecular ions in the mass spectra were in agreement with the proposed molecular formula of the compounds. The ligand spectrum gave two dominant *m/z* signals of

353 and 375 for $[M + H]^+$ and $[M + Na]^+$, respectively, which are in agreement with a calculated value of 352. ESI-MS of the complexes gave dominant *m/z* signals at 483.0, 486.9 and 482.0, which corresponded to the vcalculated values of 482.3, 487.0 and 482.0 and for nickel, copper, cobalt, complexes, respectively. Other signals were presumable due to un-identified fragments of the main compound. Furthermore, the results of the elemental analysis supported the proposed elemental composition of the compounds, as their calculated and experimental values were close juxtaposition.

4.4 | Infrared spectra of the ligand (L) and metal complexes

The FT-IR spectra of the compounds gave characteristic peaks that can be used to give credence to the formation of the compounds and fathom the coordination modes of the ligands. The IR spectra of the compounds are presented as supplementary materials (**S7–S10)**. The band at 3472 cm^{-1} in the spectrum of the ligand is attributable to the stretching vibration of the O-H group. The band was seen within 3411–3414 cm^{-1} in the spectra of the complexes, indicating the non-participation of the O-H group in the coordination. Bands at 1713 and 1672 cm^{-1} were assigned to the stretching vibrations of carbonyl (>C=O) groups in the ligand. However, the bands were seen at a lower wavenumber in the metal complexes, presumably, due to the participation of one of the carbonyl oxygen atoms in coordination to the metal ion. In addition, the stretching vibration of the azomethine group at 1628 cm^{-1} was observed at a higher wave number, in the spectra of the metal complexes (1630–1638 cm^{-1}). This increase is likely due to coordination of the nitrogen atom of one of the imine groups to the metal ion. Additional vibration peaks were observed in the spectra of the complexes within the ranges of 477–482 cm^{-1} and 502–575 cm^{-1}, due to M-O and M-N vibrations, respectively. These bands were due to the coordination of nitrogen atom of the azomethine group and one of the carbonyl oxygen, to the metal ions in the complexes. These peaks were conspicuously absent in the spectra of the ligand. However, some bending vibration peaks were observed in the spectra of the compounds around 400–600 cm^{-1}. The assignment of the peaks was in accordance with other reported studies.[65,66]

4.5 | Electronic spectra, magnetic susceptibility and molar conductance

The ligand exhibited electronic absorption bands due to $\pi \rightarrow \pi^*$ and $n \rightarrow \pi^*$ transitions, ascribed to the presence of aromatic ring and electronegative atoms. The bands at 229 and 247 nm in the ultraviolet spectrum of the ligand were assigned to the $n \rightarrow \pi^*$ and $\pi \rightarrow \pi^*$ transitions, respectively. These bands were seen at lower or higher wavelengths in the spectra of the metal complexes, because of electronic changes due to the coordination of the ligand to the metal ions.[67] The visible region of the electronic spectrum of the nickel complex gave a band at 414 nm, due to $^1Ag \rightarrow {}^1Eg$ transition, which is characteristic of a square planar geometry. The assignment of this geometry was supported by the magnetic moment value of 0.14 BM, since a moment less than 1 BM is expected for nickel complex in a square planar environment.[68] The visible spectrum of the cobalt complex gave a band at 405 nm, due to $^4A_2 \rightarrow {}^4T_1(F)$ transitions, which is characteristic of a tetrahedral geometry. The assignment of this geometry was supported by the magnetic moment value of 4.35 BM. The μeff of Co(II) complexes are expected to be higher than spin-only value for tetrahedral complexes, due to orbital contributions, and could be within the range of 4.20–4.60 BM.[69]

The copper complex gave a band in the visible region of the spectrum, at 404 nm, due to *d-d* transition. A mononuclear copper complex was confirmed with the magnetic moment of 1.98 BM. Mononuclear Cu(II) complexes have magnetic moments in the range of 1.9–2.2 BM,[70] which is usually higher than the spin-only value of 1.73 BM, due to orbital contribution and spin–orbit coupling.[71] Hence, the copper complex was assigned a tetrahedral geometry.

The molar conductance results of the complexes in DMSO showed that the complexes were non-electrolytes. According to standard Geary reference, 23–45 $\Omega^{-1}cm^2mol^{-1}$ is the expected range for 1:1 electrolytes, while below that range represents non-electrolytes.[72] The molar conductance of the metal complexes in DMSO were 14.01, 6.11 and 11.56 $\Omega^{-1}cm^2mol^{-1}$, for Ni(II), Cu(II) and Co(II) complexes, respectively.

5 | BIOLOGICAL STUDIES

5.1 | DNA binding studies

5.1.1 | UV titrations of the ligand and the complexes

The biological activities of the ligand and the complexes were investigated by UV titration method and the results are shown in Figure 1. Some hypochromicity, at 360-380 nm, were observed in the UV spectrum of the ligand, upon titration with CT-DNA (Figure 1A). This change in the spectrum indicated that the ligand, almost, did

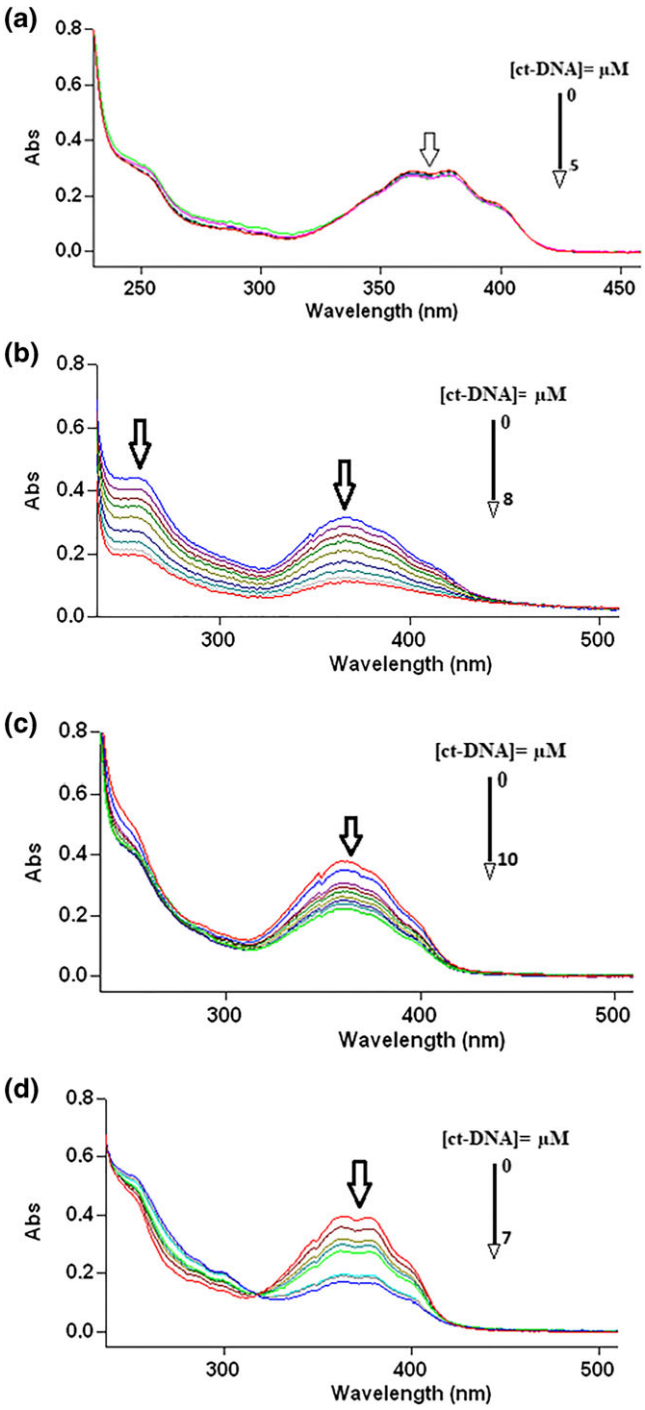

FIGURE 1 Absorption Spectra of the Ligand and Complexes in 5 mM Tris–HCl buffer (pH 7.5), upon the addition of CT-DNA. The concentration of; A: [L], B: [$CuLCl_2$], C: [$NiLCl_2$], D: [$CoLCl_2$] = 20 μM, [DNA] = 0–5 μM. Arrow shows the absorbance changing upon the increase of DNA concentration

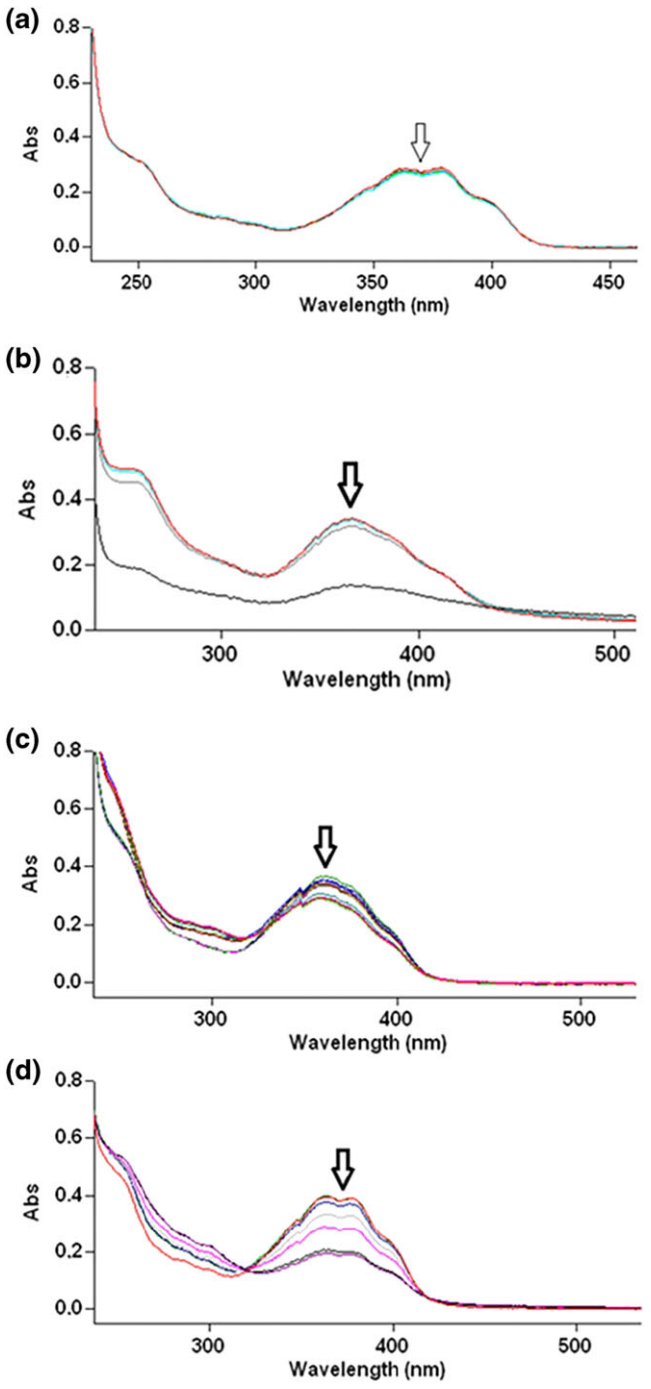

FIGURE 2 Stability of the Ligand and Complexes. The change in Absorption spectra of; A: L, B: [CuLCl2], C: [$NiLCl_2$], D: [$CoLCl_2$] in 5-mM Tris–HCl buffer (pH 7.5). Spectra were recorded in 5 min intervals, for an hour

not interact with the DNA. On the other hand, the hypochromicity around 370–385 nm, observed in the UV spectrum of the complexes (Figure 1 B-D), upon addition of the DNA, indicated that the complexes were clearly absorbed by the DNA. This may be due to an interaction between each complex and the DNA molecule. This kind of behavior in the UV spectrum may suggest that the aromatic naphthalene moiety of the complex intercalated between the base pairs, or an insertion of the whole complex in the grooves of the DNA, via H-bonds, with carboxyl and hydroxyl groups of the ligand.

The stability of the ligand and complexes were studied, using UV analysis against time frame in that the DNA titrations completed. A large degree of decrease could be seen in the spectra of copper and cobalt complexes, within an hour (Figure 2B and 2D), indicating that these complexes were not stable in the buffer solution, and they, probably, hydrolyzed. The slight change in the absorption spectrum of the ligand and nickel complex (Figure 2A and 2C) indicated a reasonably better stability for these molecules, compared to the copper and cobalt complexes. Therefore, it is observably difficult to decide to mention such interaction in the cases of the copper and cobalt complexes.

In order to quantitatively compare the DNA-binding affinities of the ligand and the complexes, the intrinsic binding constants, K_b, of the complexes to the DNA were obtained by monitoring the changes of the $\pi - \pi^*$ absorbance at 375 nm, for complexes, respectively, according to equation 2 below.

$$[\mathrm{DNA}]/(\varepsilon_A - \varepsilon_f) = [\mathrm{DNA}]/(\varepsilon_B - \varepsilon_f) + 1/K_b\,(\varepsilon_B - \varepsilon_f) \quad (2)$$

Where [DNA] is the concentration of the nucleic acid in base-pairs; ε_A is the apparent absorption coefficient, obtained by calculating A_{obs}/[Drug]; and ε_f and ε_B are the absorption coefficients for the free and the fully-bound compounds, respectively. In the $[\mathrm{DNA}]/(\varepsilon_a - \varepsilon_f)$ versus [DNA] plot, K_b is given by the ratio of the slope to the intercept.

The ligand had no affinity, while the complexes had similar moderate affinities (Table 1) for the DNA structure, comparable to some other complexes in literature.[39,73,74] This may be due to cationic nature of the complex molecules, causing them to be attracted to the negatively charged DNA. In addition to some degree of electrostatic interaction, the naphthalene moiety of the ligand may intercalate into the base pairs of the DNA molecule, or, the carbonyl and hydroxyl groups of the ligand may be H-bonded to the hetero-atoms of the bases of the DNA grooves, to achieve such moderate binding activity.

TABLE 1 Binding Constants for the Ligand and the Complexes, according to the UV Titration Experiments

Complexes	Binding constants (K_b)
L	-
$[CuLCl_2]$	1.4 x 10^5 M^{-1}
$[NiLCl_2]$	1.5 x 10^5 M^{-1}
$[CoLCl_2]$	1.4 x 10^5 M^{-1}

5.2 | Cleavage of pBR322 DNA by the complexes

The potential of the complexes to cleavage DNA was studied by gel electrophoresis, using supercoiled pBR322 DNA in ammonium acetate buffer (pH 7.5). When circular plasmid DNA is subjected to gel electrophoresis, relatively fast migration will be observed for the intact supercoil form (SC). If scission occurs on one strand the supercoil will relax to generate a slower moving open circular form (OC). If both strands are cleaved, a linear form that migrates between forms SC and OC will be generated.[73] Figure 3 shows gel electrophoresis separation of pBR322 after incubation with each of the complexes' increasing concentrations, and also, with the addition of peroxide solution. The Cu(L) complex showed some degree of DNA activity and completely changed pBR322's SC to OC, and some degree of linear-DNA formation occurred at 10 μM and higher concentrations, in the presence of peroxide. While the amount of SC of pBR322 gradually diminished, the OC form of pBR322 plasmid-DNA increased. That indicated that the copper complex, in the presence of peroxide, successfully cleaved both DNA strands. The copper complex cleaved the DNA more efficiently in the presence of peroxide, likely due to the formation of hydroxyl free radicals. The production of hydroxyl free radical was due to the reaction between the metal complex and oxidant. Those hydroxyl radicals participated in the oxidation of the deoxyribose moiety, followed by hydrolytic cleavage of the sugar phosphate backbone.[39,74] The cobalt and nickel complexes had no effect on the DNA structure.

However, the nature of the reactive intermediates involved in the DNA-cleavage by the copper complex is not clear, yet. The rapid hydrolysis of the complex must be kept in mind. Further studies on the mechanism are currently on-going.

0 concentration is for control (DNA alone); DNA was incubated at 38 °C for 1 hr with increasing concentrations (1, 10, 100 μM) of the complexes, in the absence and presence of peroxide.

5.3 | Antimicrobial screening

The identified MIC values of the ligand and complexes were as shown in Table 2. MIC of control microorganism (*Escherichia coli* ATCC 25922) was 0.03 μg mL^{-1}, for cefotaxime (expected value is 0.03–0.125 μg mL^{-1}).

All the complexes showed moderate activities to the microorganisms tested. The highest activity was observed against *S. aureus* by the copper complex, $[CuLCl_2]$.

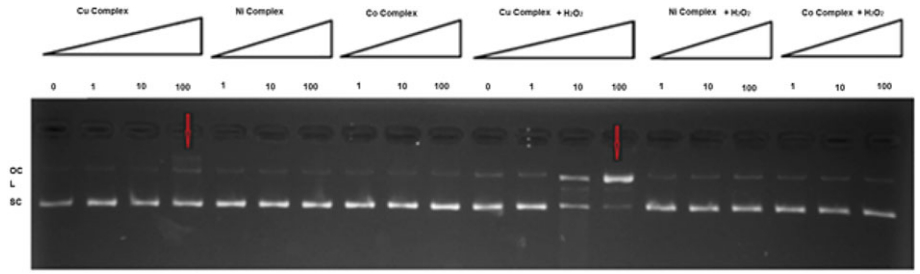

FIGURE 3 Cleavage of pBR322 DNA with Increasing Concentration of (Cu/Ni/Co) Complexes, 0 concentration is for control (DNA alone) and (DNA in the presence of peroxide); DNA was incubated at 38 °C for 1 hr with increasing concentrations (1, 10, 100 μM) of the complexes, in the absence and presence of peroxide

TABLE 2 Identified MIC Values (μg mL^{-1}) of the Complexes. (1 and 2 indicate two independent experimental results)

	Staphylococcus aureus		*Enterococcus faecalis*		*Escherichia Coli*		*Pseudomonas aeruginosa*	
	ATCC 29213		*ATCC 29212*		*ATCC 25922*		*ATCC 27853*	
	1	**2**	**1**	**2**	**1**	**2**	**1**	**2**
L	15.62	15.62	62.50	15.62	62.50	31.25	62.50	31.25
[$CuLCl_2$]	3.90	3.90	62.50	62.50	62.50	62.50	62.50	62.50
[$NiLCl_2$]	31.25	62.50	62.50	31.25	62.50	62.50	62.50	62.50
[$CoLCl_2$]	15.62	7.80	62.50	31.25	62.50	62.50	62.50	62.50

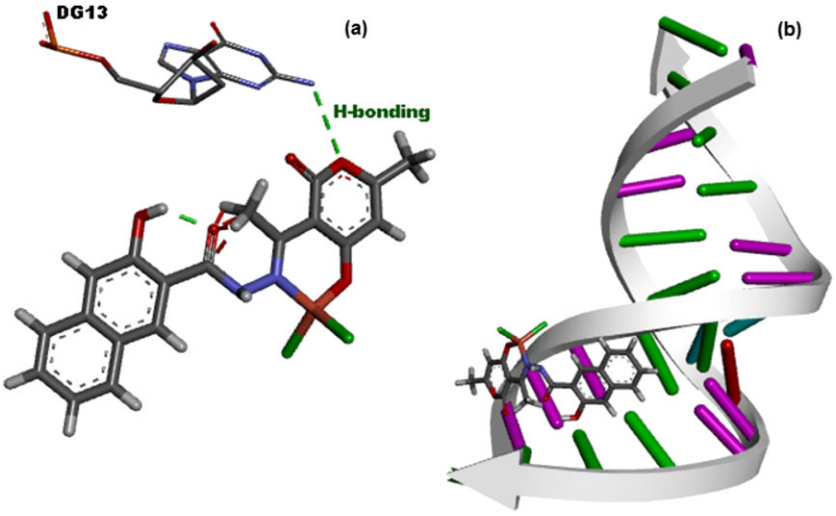

FIGURE 4 Representation of 3-D **(a)** and 2-D **(b)** hydrogen bonding interactions inside the active pocket of A-DNA-Cu complex

5.4 | Molecular docking

Molecular docking studies were performed to provide insights to the interactions between complexes and A-DNA. Docking results within the Root Mean Square Deviation (RMSD) value of 2 Å are considered acceptable.[75] The RMSD values of all the complexes were below 2 Å. The docking experiment performed on the complexes, with A-DNA tetradecanucleotide sequence, d (CCCCGGTACCGGGG)2, with $C_2{\cdot}G_{13}$ base-pair,

TABLE 3 Binding Affinities (kcal mol^{-1}) of the Complexes with A-DNA and Antimicrobial Enzymes Obtained from Docking Experiment

Complexes	*A-DNA*	*Staphylococcus aureus*	*Enterococcus faecalis*	*Escherichia coli*	*Pseudomonas aeruginosa*
[$CoLCl_2$]	−8.2	−6.4	−5.2	−5.4	−4.5
[$CuLCl_2$]	−8.9	−10.5	−5.4	−4.5	−4.4
[$NiLCl_2$]	−8.0	−7.6	−5.3	−4.4	−4.3

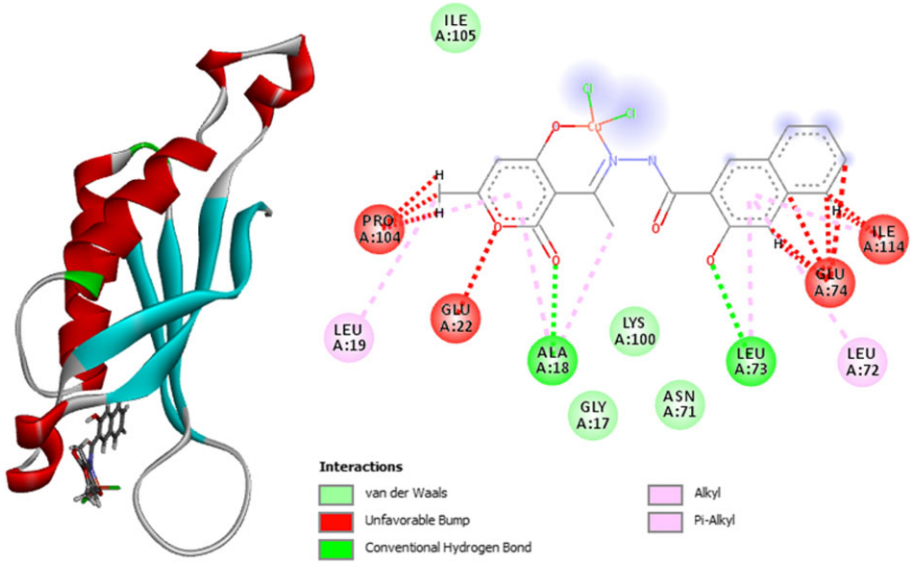

FIGURE 5 Representation of 3-D (a) and 2-D (b) The amino acid residues involved in interactions with $[CuLCl_2]$ inside the active pocket of *Staphylococcus aureus* (PDB: 2DHN with 2.2 Å resolution)[43]

identified the major groove as the binding side.[42,76] As seen in Figure 4, the most favorable, energetically docked pose[77] revealed that $[CuLCl_2]$ bound to the major groove ($C_2{\cdot}G_{13}$ base-pair) (DG13) of the A-DNA through the pyran ring, while $[CoLCl_2)]$ and $[NiLCl_2]$ were found around the minor groove (supplementary material, Figure S11). The binding of $[CuLCl_2]$, through hydrogen bonding (Figure 4), in the major groove, leads to the stability of the groove.[77,78] The binding energy for the docking experiment (Table 3) was found to be −8.9 kcal mol^{-1} for $[CuLCl_2]$, though the difference in energy compared to $[CoLCl_2]$ and $[NiLCl_2]$ was about −0.7 and − 0.9

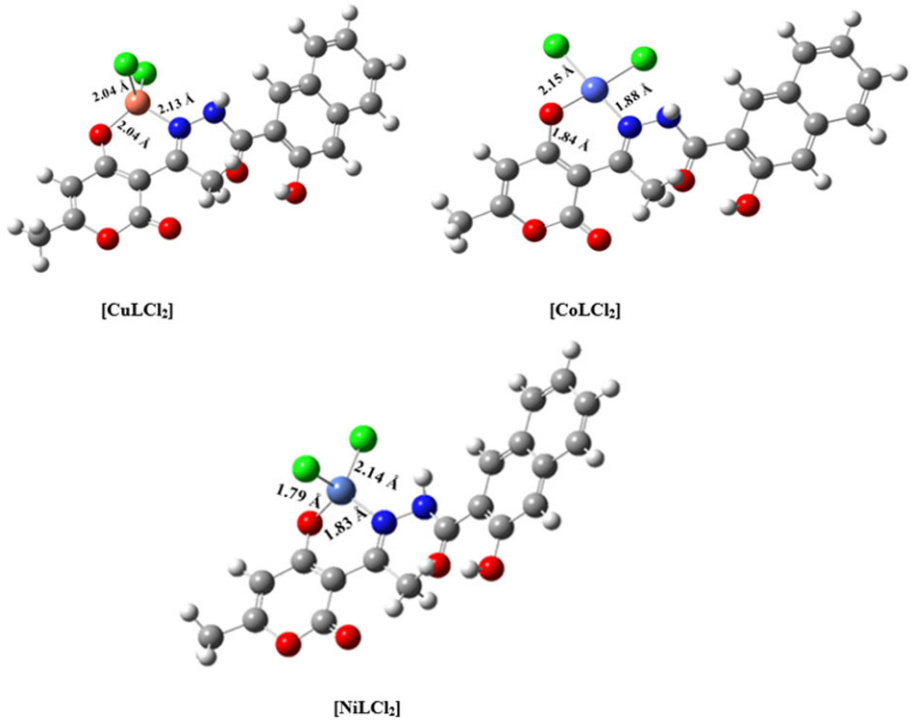

FIGURE 6 DFT-Optimized Structures of Complexes with the Key Interatomic Distances Obtained at B3LYP/6–31 + G(d,p) and LANL2DZ for the Metal Complexes

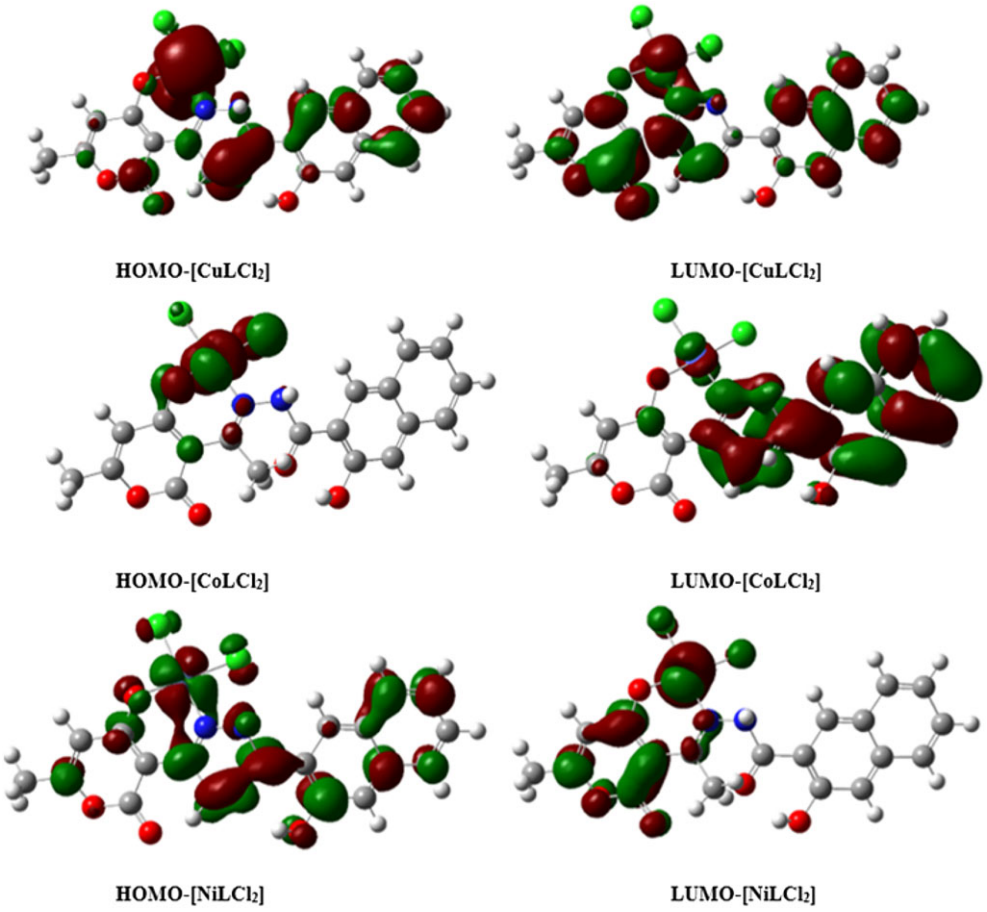

FIGURE 7 HOMO-LUMO Diagram Representing the Distribution of Electron Delocalization Obtained at B3LYP/6–31 + G(d,p)/LANL2DZ

kcal mol^{-1} respectively. The highest binding energy of $[CuLCl_2]$ explained the experimental finding as to why copper complex cleaved DNA more efficiently, compared to the other complexes.

Antimicrobial docking experiment was also carried out to know the inhibitory effects of the complexes on Gram-positive (S. *aureus* and *Enterococcus faecalis*) and Gram-negative (E. *coli*, P. *aeruginosa*) bacteria. As shown in Table 3, $[CuLCl_2]$ was found as the most effective on Gram-positive bacteria, with an indicative highest affinity for S. *aureus,* with −10.5 kcal mol^{-1}. From Figure 5, it is seen that the $[CuLCl_2]$ complex binding showed the formation of hydrogen bonding with the active-site amino acid residues (ALA18, LEU73), and Van der Waals interactions involving LYS100 and GLY17 of S. *aureus* (2DHN).[43] These agreed with the experimental findings, and would provide more information on groove binding and antimicrobial inhibition, towards computer-aided drug discovery.

6 | DFT ANALYSIS

6.1 | Optimized geometries

The DFT-optimized geometries, with the key interatomic distances, in Angstrom, of $[CuLCl_2]$, $[CoLCl_2]$ and $[NiLCl_2]$ complexes are shown in Figure 6. The metal–ligand distances obtained were similar to literature-reported metal–ligand distances.[63,79]

TABLE 4 Calculated E_{HOMO}, E_{UMO}, ΔE of the Complexes, Obtained at B3LYP/6–31 + G(d,p)/LANL2DZ

Complex	E_{HOMO} (eV)	E_{LUMO} (eV)	ΔE (eV)
$[CuLCl_2]$	−6.20	−4.96	1.24
$[CoLCl_2]$	−5.27	−3.35	1.92
$[NiLCl_2]$	- 6.15	−4.42	1.73

TABLE 5 Thermodynamic Properties of the Complexes, Obtained at B3LYP/6–31 + G(d,p)/LANL2DZ

Complex	ΔH (kJ/mol)	ΔG (kJ/mol)	ΔS (J/mol/K)
$[CuLCl_2]$	−526.11	−649.4	126.29
$[CoLCl_2]$	−656.32	−790.43	134.11
$[NiLCl_2]$	−611.64	−985.72	128.88

6.2 | FMO and thermodynamic analysis

HOMO and LUMO are also regarded as the frontier molecular orbitals.[58,80] The electron-donating ability of a complex is associated with the E_{HOMO}; the higher the E_{HOMO} energies (less negative), the more energy, implying more ability to donate electrons.[63,81] The distribution of electrons of the HOMO (Figure 7) is prominent in the $[CuLCl_2]$ complex, compared to Co and Ni complexes. All the complexes showed low ΔE (E_{LUMO} - E_{HOMO}) gap, signifying a high chemical reactivity (Table 4). The lower ΔE of $[CuLCl_2]$ indicated higher tendency for electrons to move to the excited state, and a higher tendency to donate electron to an electron-accepting species, compared to $[CoLCl_2]$ and $[NiLCl_2]$.

6.3 | All energies were corrected for zero-point energy contributions

The thermodynamic properties of the complexes are shown in Table 5. Entropy is the degree of disorderliness of a system.[63,82,83] Positive entropy designates increase in randomness in a system, and aids favorable formation of the complex.[84] The order of entropy increase is $[CuLCl_2] < [NiLCl_2]$ $[CoLCl_2]$. The measure of (more negative) ΔG is an indication of the stability of the system,[84] and also shows the degree of spontaneity of a process.[54,84,85] The ΔG value (negative) of all the metal complexes displayed spontaneous formation, with $[NiLCl_2]$ exhibiting higher stability (highest negative ΔG value) than others. The enthalpy (ΔH) values of the complexes suggested the formation of non-covalent interactions between atoms within the complexes.[84]

6.4 | ^{1}H-NMR Spectrum analysis

The calculated ^{1}H-NMR spectrum for the ligand is presented in the supplementary material, Figure S12. Significant hydrogen atoms were indicated in the calculated ^{1}H-NMR spectrum. The DFT result for the ^{1}H-NMR obtained showed good agreement with experimental ^{1}H-NMR chemical shifts, with a small deviation of 0.04 and 0.06 ppm for H14 and H15, respectively. H10 and H18 displayed slightly larger deviations of 0.16 and 0. 36 ppm, respectively. Our results, with regards to the deviations from the experimental values, were comparable to those reported previously for DFT ^{1}H-NMR calculations.[62]

7 | CONCLUSION

The investigation has demonstrated the successful syntheses and spectroscopic characterization of a novel hydrazone of naphthoic hydrazide and dehydroacetic acid, and its Cu(II), Co(II), Ni(II) complexes. Antibacterial and DNA cleavage properties, molecular docking and DFT results indicated that the Cu(II) complex had the highest activity against *S. aureus,* and cleaved DNA more efficiently than the Ni(II) and Co(II) complexes. In future, we intend to further investigate the antipathogenic and DNA cleavage potentials of other derivatives of the same ligand and their complexes.

ACKNOWLEDGMENTS

The authors thank the University of Nigeria, Nsukka, Ikwo, Zonguldak Bulent Ecevit University, Zonguldak and University of KwaZulu-Natal, Durban for operational and infrastructural support. OTU thank Ekele Dinneya-Onuoha of the Department of Pure and Industrial Chemistry, University of Nigeria, Nsukka for Technical support.

ORCID

Anthony C. Ekennia https://orcid.org/0000-0002-3324-7566
Ilknur Babahan https://orcid.org/0000-0001-6081-4899
Burak Coban https://orcid.org/0000-0003-1401-668X
Oguejiofo T. Ujam https://orcid.org/0000-0002-5628-209X

REFERENCES

[1] J.-Y. Miao, *Synth. React. Inorg. Met-Org. And Nano-Metal Chem.* **2012**, *42*, 1463.

[2] Ł. Popiołek, I. Piątkowska-Chmiel, M. Gawrońska-Grzywacz, A. Biernasiuk, M. Izdebska, M. Herbet, M. Sysa, A. Malm, J. Dudka, M. Wujec, *Biomed. Pharmacother.* **2018**, *103*, 1337.

[3] H. D. Yin, S. W. Chen, *Inorg. Chim. Acta* **2006**, *359*, 3330.

[4] H. N. Dogan, A. Duran, S. Rollas, *Indian J. Chem.* **2005**, *44B*, 2301.

[5] S. Khattab, *Molecules* **2005**, *10*, 1218.

[6] A. Duran, H. N. Dogan, S. Rollas, *Farmaco* **2002**, *57*, 559.

[7] H. N. Dogan, S. Rollas, H. Erdeniz, *Farmaco* **1998**, *53*, 462.

[8] H. N. Dogan, A. Duran, S. Rollas, G. Sener, M. K. Uysal, D. Gulen, *Bioorg. Med. Chem.* **2002**, *10*, 2893.

[9] A. M. Khalil, M. A. Berghot, M. A. Gouda, *J. Saudi Chem. Soc.* **2016**, *20*, 165.

[10] L. S. Kumar, K. S. Prasad, H. D. Revenasiddappa, *Eur. J. Chem.* **2011**, *2*, 394.

[11] G. Nöhammer, *Histochem.* **1990**, *94*, 485.

[12] G. K. Gupta, A. Mittal, V. Kumar, *Letters Org. Chem.* **2014**, *11*, 273.

[13] A. Kumar, P. Lohan, D. K. Aneja, G. K. Gupta, D. Kaushik, O. Prakash, *Eur. J. Med. Chem.* **2012**, *50*, 81.

[14] R. Pal, V. Kumar, V. Beniwal, G. K. Gupta, A. K. Gupta, *Der Pharma Chemica* **2014**, *6*, 31.

[15] D. Kumar, P. Sharma, H. Singh, K. Nepali, G. K. Gupta, S. K. Jaina, F. Fidele Ntie-Kang, *RSC Adv.* **2017**, *7*, 36977.

[16] A. Kumar, R. Prakash, S. P. Singh, *Synth. Commun.* **2005**, *35*, 461.

[17] O. Kumar, O. Prakash, M. Kinger, S. P. Singh, *Can. J. Chem.* **2006**, *84*, 438.

[18] O. Prakash, A. Kumar, A. Sadana, S. P. Singh, *Synth. Commun.* **2002**, *32*, 2663.

[19] O. Prakash, A. Kumar, S. P. Singh, *J. Indian Chem. Soc.* **2003**, *80*, 1035.

[20] O. Prakash, A. Kumar, S. P. Singh, *Heterocycles* **2004**, *63*, 1193.

[21] A. K. Gupta, R. Pal, V. Beniwal, *World J. Pharm. Pharm. Sci.* **2014**, *4*, 990.

[22] R. Prakash, A. Kumar, S. P. Singh, R. Aggarwal, O. Prakash, *Indian J. Chem. Section B* **2007**, *46B*, 1713.

[23] J. D. Edwards, J. E. Page, M. Pianka, *J. Chem. Soc. (Resumed)* **1964**, 5200.

[24] R. P. Saini, V. Kumar, A. K. Gupta, G. K. Gupta, *Med. Chem. Res.* **2014**, *23*, 690.

[25] D. M. Fouad, N. M. Ismail, M. A. El-Gahami, S. A. Ibrahim, *Spectrochim. Acta Part A* **2007**, *67*, 564.

[26] E. Mikami, T. Goto, T. Ohno, H. Matsumoto, M. Nishida, *J. Pharm. Biomed. Anal.* **2002**, *28*, 261.

[27] C. Altomore, G. Perrone, M. C. Zonno, A. Evidente, R. Pengue, F. F, L. Polonelli, *J. Nat. Prod.* **2000**, *63*, 1131.

[28] C. Altomore, R. Pengue, M. Favilla, A. Evidente, A. Visconti, *J. Agric. Food Chem.* **2004**, *52*, 2997.

[29] N. Raman, S. Thalamuthu, J. D. Raja, M. A. Neelakandan, S. Banerjee, *J. Chil. Chem. Soc.* **2008**, *53*, 1439.

[30] S. Grguric-Sipka, R. Vilaplana, J. Perez, M. Fuertes, C. Alonso, T. Alvarez, T. Sabo, F. Gonzalez-Vilchez, *J. Inorg. Biochem.* **2003**, *97*, 215.

[31] N. N. Ljubijankić, A. A. Zahirović, E. E. Turkušić, E. E. Kahrović, *Croat. Chem. Acta* **2013**, *86*, 215.

[32] S. Rauf, J. Gooding, K. Akhtar, M. Ghauri, M. Rahman, M. Anwar, A. Khalid, *J. Pharm. Biomed. Anal.* **2005**, *37*, 205.

[33] A. A. Olanrewaju, C. U. Ibeji, F. S. Fabiyi, *Indian J. Heterocyc. Chem.* **2018**, *28*, 351.

[34] J. Jayabharathi, V. Thanikachalam, K. Jayamoorthy, M. V. Perumal, *Spectrochim. Acta A: Mol. Biomol. Spectrosc.* **2011**, *79*(6).

[35] B. Coban, I. O. Tekin, A. Sengul, U. Yildiz, I. Kocak, N. Sevinc, *J. Biol. Inorg. Chem.* **2016**, *21*, 163.

[36] L. Patiny, A. Borel, *J. Chem. Inf. Model.* **2013**, *53*, 1223.

[37] N. J. A. Coughlan, W. Henderson, *J. Coord. Chem.* **2014**, *67*, 3987.

[38] B. Atabey-Ozdemir, O. Demirkiran, U. Yildiz, I. O. Tekin, B. Coban, *Bulgarian Chem. Commun.* **2017**, *49*, 901.

[39] B. Coban, N. Eser, I. Babahan, *Bulgarian Chem. Commun.* **2017**, *49*, 908.

[40] *Methods for Dilution Antimicrobial Susceptibility Tests for Bacteria That Grow Aerobical Approved Standard*, 10th ed., CLSI document M07/−A10, Clinical Laboratory Standarts Institute, Wayne, PA **2015**.

[41] O. Trott, A. J. Olson, *J. Comput. Chem.* **2010**, *31*, 455.

[42] P. K. Mandal, S. Venkadesh, N. Gautham, *Acta Crystallogr. Section F: Struct. Bio. Crystal. Commun.* **2012**, *68*, 393.

[43] M. Hennig, D. Allan, I. C. Hampele, M. G. Page, C. Oefner, G. E. Dale, *Nature Struct. Mol. Bio.* **1998**, *5*, 357.

[44] A. Pan, A. M. Balakrishna, W. Nartey, A. Kohlmeier, P. V. Dip, S. Bhushan, G. Grüber, *Free Radical Bio. Med.* **2018**, *115*, 252.

[45] D. Systemes, Dassault Systemes: San Diego, CA **2015**.

[46] R. Jauch, A. Humm, R. Huber, M. C. Wahl, *J Biol. Chem.* **2005**, *280*, 15131.

[47] K. Remans, K. Pauwels, P. van Ulsen, L. Buts, P. Cornelis, J. Tommassen, S. N. Savvides, K. Decanniere, P. Van Gelder, *J. Mol. Biol.* **2010**, *401*, 921.

[48] M. F. Sanner, *J. Mol. Graphics Modell.* **1999**, *17*, 57.

[49] G. M. Morris, R. Huey, W. Lindstrom, M. F. Sanner, R. K. Belew, D. S. Goodsell, A. J. Olson, *J. Comput. Chem.* **2009**, *30*, 2785.

[50] M. J. Frisch, G. W. Trucks, H. B. Schlegel, G. E. Scuseria, M. A. Robb, J. R. Cheeseman, G. Scalmani, V. Barone, B. Mennucci, G. A. Petersson, H., Nakatsuji, M. Caricato, X. Li, H. P. Hratchian, A. F. Izmaylov, J. Bloino, G. Zheng, J. L. Sonnenberg, M. Hada, M. Ehara, K. Toyota, R. Fukuda, J. Hasegawa, M. Ishida, T. Nakajima, Y. Honda, O. Kitao, H. Nakai, T. Vreven, J. A. Montgomery Jr., J. E. Peralta, F. Ogliaro, M. Bearpark, J. J. Heyd, E. Brothers, K. N. Kudin, V. N. Staroverov, R. Kobayashi, J. Normand, K. Raghavachari, A. Rendell, J.C. Burant, S. S. Iyengar, J. Tomasi,M. Cossi, N. Rega, J. M. Millam, M. Klene, J. E. Knox, J. B. Cross, V. Bakken, C. Adamo, J. Jaramillo, R. Gomperts, R. E. Stratmann, O. Yazyev, A. J. Austin, R. Cammi, C. Pomelli, J. W. Ochterski, R. L. Martin, K. Morokuma, V. G. Zakrzewski, G. A. Voth, P. Salvador, J. J. Dannenberg, S. Dapprich, A. D. Daniels, Ö. Farkas, J.B. Foresman, J. V. Ortiz, J. Cioslowski, Fox, D. J. Gausn, Revision E.01, Inc., Wallingford CT, **2009**.

[51] O. A. Oyebode, O. L. Erukainure, C. I. Chukwuma, C. U. Ibeji, N. A. Koorbanally, S. Islam, *Biomed. Pharmacother.* **2018**, *106*, 1116.

[52] M. M. Makatini, K. Petzold, C. N. Alves, P. I. Arvidsson, B. Honarparvar, P. Govender, T. Govender, H. G. Kruger, Y. Sayed, J. Lameira, *J. Enzyme Inhibit. Med. Chem.* **2013**, *28*, 78.

[53] A. D. Becke, *J. Chem. Phy.* **1992**, *96*, 2155.

[54] A. C. Ekennia, A. A. Osowole, L. O. Olasunkanmi, D. C. Onwudiwe, O. O. Olubiyi, E. E. Ebenso, *J. Mol. Struct.* **2017**, *1150*, 279.

[55] B. Tang, J.-H. Ye, X.-H. Ju, *ISRN Org. Chem.* **2011**, *2011*, 1.

[56] S. I. Gorelsky, L. Basumallick, J. Vura-Weis, R. Sarangi, K. O. Hodgson, B. Hedman, K. Fujisawa, E. I. Solomon, *Inorg. Chem.* **2005**, *44*, 4947.

[57] L. Chen, T. Liu, C. A. Ma, *J. Phy. Chem. A* **2009**, *114*, 443.

[58] S. M. A. Rauf, P. I. Arvidsson, F. Albericio, T. Govender, G. E. Maguire, H. G. Kruger, B. Honarparvar, *Org. Biomol. Chem.* **2015**, *13*, 9993.

[59] Z. Fakhar, T. Govender, G. Lamichhane, G. E. M. Maguire, H. G. Kruger, B. Honarparvar, *J. Mol. Struct.* **2017**, *1128*, 94.

[60] K. Wolinski, J. F. Hinton, P. Pulay, *J. Am. Chem. Soc.* **1990**, *112*, 8251.

[61] E. Cances, B. Mennucci, J. Tomasi, *J. Chem. Phy.* **1997**, *107*, 3032.

[62] L. A. De Souza, W. M. Tavares, A. P. M. Lopes, M. M. Soeiro, W. B. De Almeida, *Chem. Phy. Letters* **2017**, *676*, 46.

[63] A. C. Ekennia, A. A. Osowole, D. C. Onwudiwe, I. Babahan, C. U. Ibeji, S. N. Okafor, O. T. Ujam, *Applied Organomet. Chem.* **2018**, *32*, e4310.

[64] C. S. Anitha, S. Sumathi, P. Tharmaraj, C. D. Sheela, *Inter. J. Inorg. Chem.* **2011**, *8*.

[65] K. Z. Ismail, *Trans. Met. Chem.* **2000**, *25*, 522.

[66] A. A. Ekennia, A. A. Osowole, L. O. Olasunkanmi, D. C. Onwudiwe, E. E. Ebenso, *Res. Chem. Intermed.* **2017**, *43*, 3787.

[67] S. M. E. Khalil, H. S. Seleem, B. A. El-Shetary, M. Shebl, *J. Coord. Chem.* **2002**, *55*, 883.

[68] D. C. Onwudiwe, A. C. Ekennia, E. Hosten, *J. Coord. Chem.* **2016**, *69*, 2454.

[69] F. A. Cotton, G. Wlkinson, C. A. Murillo, M. Bochmann, *Advanced Inorganic Chemistry*, 6th ed., John Wiley, New York **1999**.

[70] T. L. Yang, W. W. Qin, *Polish J. Chem.* **2006**, *80*, 1657.

[71] A. A. Osowole, R. Kempe, R. Schobert, K. Effenberger, *Metal-Org. Nano-Metal Chem.* **2011**, *41*, 825.

[72] W. J. Geary, *Coord. Chem. Reviews* **1971**, *7*, 81.

[73] J. K. Barton, A. L. Raphael, *J. Am. Chem. Soc.* **1984**, *106*, 2466.

[74] J. Borowska, M. Sierant, E. Sochacka, D. Sanna, E. Lodyga-Chruscinska, *J. Biol. Inorg. Chem.* **2015**, *20*, 989.

[75] B. Kramer, M. Rarey, T. Lengauer, *Proteins: Struct. Funct. Bioinform.* **1999**, *37*, 228.

[76] C. A. Bingman, G. Zon, M. Sundaralingam, *J. Mol. Bio.* **1992**, *227*, 738.

[77] F. Arjmand, S. Parveen, M. Afzal, M. Shahid, *J. Photochem. Photobio. B: Biology* **2012**, *114*, 15.

[78] R. Filosa, A. Peduto, S. Di Micco, P. de Caprariis, M. Festa, A. Petrella, G. Capranico, G. Bifulco, *Bioorg. Med. Chem.* **2009**, *17*, 13.

[79] A. Nimmermark, L. Öhrström, J. Reedijk, *Zeitschrift für Kristallogr.-Crystal. Mat.* **2013**, *228*, 311.

[80] R. S. Dumont, *Canadian J. Chem.* **2013**, *92*, 100.

[81] C. U. Ibeji, I. A. Adejoro, B. B. Adeleke, *J. Phy. Chem. Biophy.* **2015**, *5*, 193.

[82] I. M. Alecu, J. Zheng, Y. Zhao, D. G. Truhlar, *J. Chem. Theory Comput.* **2010**, *6*, 2872.

[83] M. M. Lawal, T. Govender, G. E. Maguire, H. G. Kruger, B. Honarparvar, *Int. J. Quantum Chem.* **2017**, *118*, e25497.

[84] X. Du, Y. Li, Y. L. Xia, S. M. Ai, J. Liang, P. Sang, A. L. Ji, S. Q. Liu, *Inter. J. Mol. Sci.* **2016**, *17*, 144.

[85] F. Chioma, A. C. Ekennia, C. U. Ibeji, S. N. Okafor, D. C. Onwudiwe, A. A. Osowole, O. T. Ujam, *J. Mol. Struct.* **2018**, *1163*, 455.

SUPPORTING INFORMATION

Additional supporting information may be found online in the Supporting Information section at the end of the article.

How to cite this article: Ekennia AC, Ibezim EC, Okpareke OC, et al. Novel 3-Hydroxy-2-naphthoic hydrazone and Ni(II), Co(II) and Cu(II) Complexes: Synthesis, Spectroscopic Characterization, Antimicrobial, DNA Cleavage and Computational Studies. *Appl Organometal Chem*. 2019;e4913. https://doi.org/10.1002/aoc.4913